CellPress
Gold Standard for the Global Goals
1 ton of CO_2 offset

One Earth

Review

Air-Filtering Masks for Respiratory Protection from $PM_{2.5}$ and Pandemic Pathogens

Jinwei Xu,[1] Xin Xiao,[1] Wenbo Zhang,[1] Rong Xu,[1] Sang Cheol Kim,[1] Yi Cui,[1] Tyler T. Howard,[1] Esther Wu,[1] and Yi Cui[1,2,*]
[1]Department of Materials Science and Engineering, Stanford University, Stanford, CA 94305, USA
[2]Stanford Institute for Materials and Energy Sciences, SLAC National Accelerator Laboratory, 2575 Sand Hill Road, Menlo Park, CA 94025, USA
*Correspondence: yicui@stanford.edu
https://doi.org/10.1016/j.oneear.2020.10.014

SUMMARY

Air-filtering masks, also known as respirators, protect wearers from inhaling fine particulate matter ($PM_{2.5}$) in polluted air, as well as airborne pathogens during a pandemic, such as the ongoing COVID-19 pandemic. Fibrous medium, used as the filtration layer, is the most essential component of an air-filtering mask. This article presents an overview of the development of fibrous media for air filtration. We first synthesize the literature on several key factors that affect the filtration performance of fibrous media. We then concentrate on two major techniques for fabricating fibrous media, namely, meltblown and electrospinning. In addition, we underscore the importance of electret filters by reviewing various methods for imparting electrostatic charge on fibrous media. Finally, this article concludes with a perspective on the emerging research opportunities amid the COVID-19 crisis.

INTRODUCTION

Particulate matter (PM) air pollution poses significant risks to public health and adversely affects visibility, climate, and ecosystems.[1–3] PM is categorized into $PM_{2.5}$ and PM_{10}, referring to PM with particle sizes below 2.5 and 10 μm, respectively. $PM_{2.5}$ is particularly harmful because it can penetrate into the lungs and is sometimes small enough to enter the bloodstream; therefore, long-term exposure to $PM_{2.5}$ is associated with a higher risk of lung cancer and cardiovascular disease.[4] A model[1] estimated that 8.9 million deaths in 2015 were associated with long-term exposure to $PM_{2.5}$ air pollution. Ninety-five percent of the world population live in areas with annual average concentration of $PM_{2.5}$ above the World Health Organization safe level of 10 $\mu g \cdot m^{-3}$ (Figure 1A); the situation is most dire in Central Africa, Middle East, India, and China.[5] Consequently, wearing masks has become an increasingly common method for the public to reduce their exposure to air pollution, particularly in developing countries.

The ongoing COVID-19 pandemic, caused by the SARS-CoV-2 virus, has led to more than 40 million confirmed cases globally, with more than 1 million deaths, as of October 20, 2020.[7] The rapid spread of COVID-19 is driven by an important route of human-to-human transmission via viral saliva droplets (>10 μm) and aerosols (<10 μm) (Figure 1B), which are released into the air by infected individuals when they breathe, speak, cough, or sneeze.[8] Viral aerosols smaller than 5 μm in diameter are critically dangerous since they remain suspended in the air for long periods of time and can reach the lower respiratory tract of a susceptible host.[9] Therefore, air-filtering masks, such as N95 masks (also known as N95 filtering facepiece respirators), are the most essential personal protective equipment for frontline health care workers fighting the pandemic. Regarding the general public, wearing masks and social distancing have become the most effective practices to protect vulnerable people and prevent hospitals being overwhelmed when mandatory quarantine is lifted. As the ripple effect of the COVID-19 pandemic continues to unfold worldwide, wearing masks in common areas is no doubt one of the many changes to which the public need to adapt.

Although we have witnessed a dramatic decline in the anthropogenic emissions of $PM_{2.5}$ due to the travel restrictions and economic shutdowns during the COVID-19 pandemic, governments around the world have relaxed environmental regulations indefinitely to stimulate economic recovery.[10,11] In addition, commuters may adopt more polluting transportation modes out of fear of exposure to SARS-CoV-2 in crowded public transport.[12] Consequently, air pollution may overshoot the pre-pandemic level once the economy fully reopens. More significantly, numerous studies[13–16] have suggested that air pollution can increase the transmission and susceptibility of COVID-19 as well as worsen the severity of the infection. At a time of unprecedented global change, masks that protect people by filtering out $PM_{2.5}$ and airborne pathogens have never been more important. Therefore, it is necessary to write a review on the past development of air-filtering masks to identify recent progress and remaining knowledge gaps, and it is essential to envision emerging research opportunities amid the pressing challenges of air pollution and COVID-19.

A mask is usually composed of multiple layers (Figure 1C). The most essential component of a mask is the middle filtration layer, also known as the filter medium. The filtration layers of almost all masks are fibrous media, which are made up of a large number of sparsely distributed fibers that are bonded to one another. A typical cross-sectional scanning electron microscope (SEM) image of an N95 mask is shown in Figure 1D. The filtration layer is

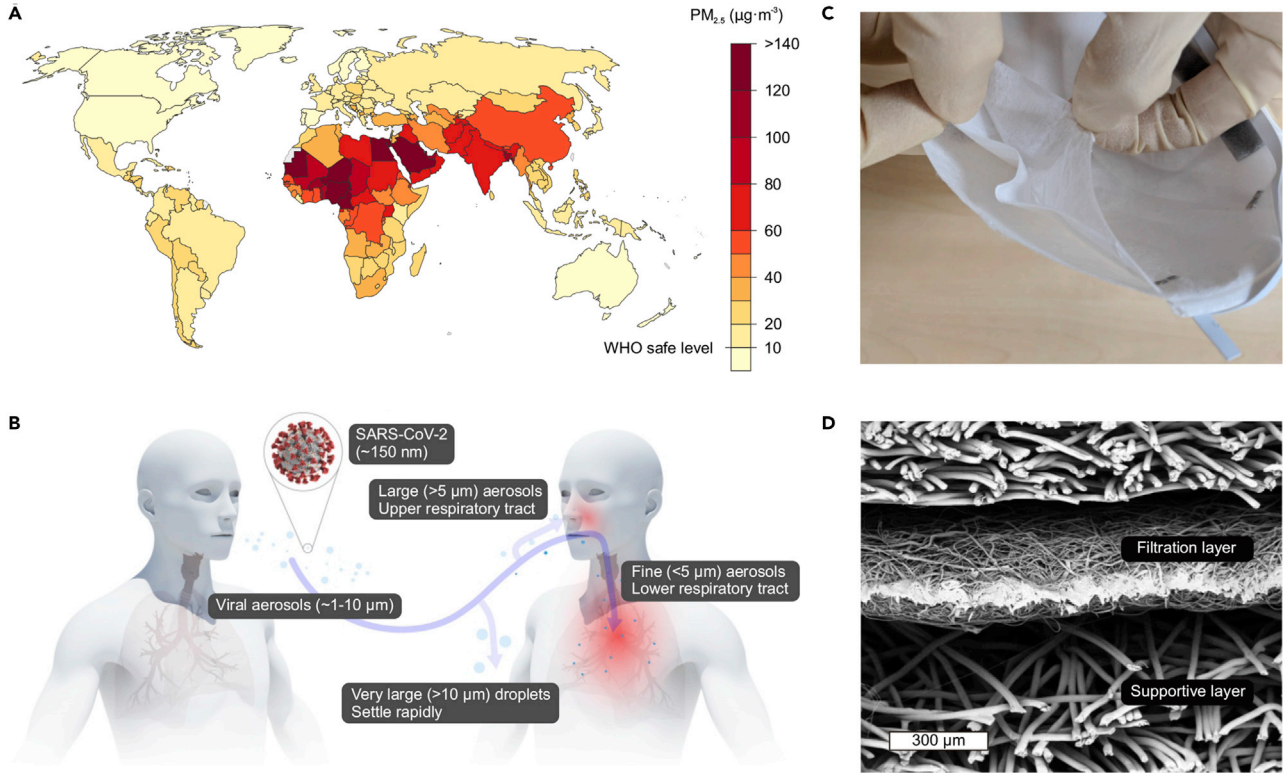

Figure 1. Masks Protecting People from $PM_{2.5}$ and Pandemic Pathogens

(A) Annual average concentration of $PM_{2.5}$ around the globe in 2016. Image courtesy of Ritchie et al.,[5] CC BY 4.0, via Our World in Data. Data source, World Bank.
(B) Transmission of the SARS-CoV-2 virus through viral aerosols.
(C) Peeling apart an N95 mask revealing multiple layers.
(D) Cross-sectional SEM image of an N95 mask showing that the filtration layer is sandwiched between the supportive layers.
(B), (C), and (D) are adapted from Liao et al.[6] with permission.

protected from abrasion by the mechanically supportive top and bottom layers. The supportive layers also add key functions to a mask (e.g., a hydrophobic outer layer to repel water, a hydrophilic inner layer to absorb moisture from respiration, skin-friendly textile to ensure wearer comfort, a rigid frame to provide fit, etc.), yet contribute little to the filtration efficiency. Due to the lack of N95 and surgical masks during the COVID-19 pandemic, individuals are encouraged to wear facial coverings made of household fabrics, which are also based on fibrous materials and have been carefully studied recently.[17,18]

Although an emphasis is put on masks here, the discussions in this review also provides a valuable reference for other air filtration applications where fibrous media play a major role, such as building ventilation, engine air filters, and industrial pollution control. The review consists of four sections. (1) We start with a summary of the key factors that affect the filtration performance of fibrous media. Both intrinsic factors, such as the material properties, and extrinsic factors, such as the environmental conditions, are included. (2) We then review the development of the two main techniques for fabricating fibrous media (i.e., melt-blown and electrospinning) and identify their advantages and disadvantages. (3) We further discuss techniques to impart electrostatic charge on fibrous media, which is the most effective strategy to improve the filtration performance. (4) We conclude with an outlook on the future development of air-filtering masks, with topics including anti-pathogens, thermal comfort, wearable electronics, and eco-friendliness.

FACTORS AFFECTING FILTRATION PERFORMANCE

Tremendous efforts have been devoted to identifying the key factors that affect the filtration performance of a fibrous medium. These key factors can be divided into two classes: (1) intrinsic factors, such as the geometric properties, the electrostatic charge density, and the chemical composition of the fibrous medium, and (2) extrinsic factors, such as inhalation flow rate, humidity, and long-term storage. The relationships between these key factors and the filtration performance serve as guidelines for the development and design of filter media. In this section, we first give a brief summary of filtration mechanisms, which provides the foundation for the further discussion. We then review the effects of the key factors as mentioned above on the filtration performance. In view of the COVID-19 pandemic, we also provide a discussion on the effect of different sterilization methods on the filtration performance at the end of this section.

Filtration Mechanisms

The single-fiber model[19,20] is the most prevalent model for air filtration; although we would like to point out that this simple model is insufficient, and there is a good amount of work on

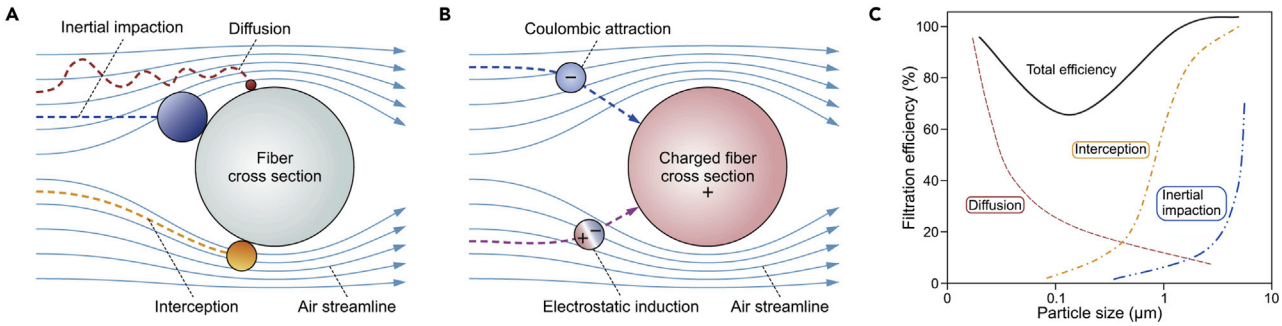

Figure 2. Filtration Mechanisms

(A) Schematic illustration of the single-fiber model. Inertial impaction, interception, and diffusion are collectively known as mechanical filtration mechanisms.
(B) Electrostatic filtration mechanisms for electret filters.
(C) Contribution of each mechanism toward the total filtration efficiency. Note: Only mechanical filtration mechanisms are included here. Refer to Figure 3E for the contribution of electrostatic filtration mechanisms. Adapted from Mukhopadhyay et al.[20] with permission.

the way to translate the single-fiber model to more realistic fiber configurations.[21–23] The capture of a particle by an isolated fiber follows one or a combination of three mechanisms: inertial impaction, interception, and diffusion (Figure 2A). Particles larger than 10 μm rapidly settle due to gravity and are not considered here. Inertial impaction occurs when a particle has a high momentum due to a larger size (>3 μm), which allows the particle to deviate from the air streamline and impact a fiber along a straighter path. Interception applies to smaller particles (1–3 μm) that do not have sufficient inertia to break away from the air streamline. Therefore, these particles can only be captured when the air streamlines that they follow are close enough to a fiber. Diffusion becomes the dominant mechanical capture mechanism for very fine particles (<1 μm). These particles can move across air streamlines by Brownian motion, which greatly enhances the probability of their collision with fibers.

Two more filtration mechanisms, Coulombic attraction (or repulsion) and electrostatic induction (Figure 2B), should also be considered for electret filters,[24] which are made of fibers embedded with electrostatic charge. Coulombic attraction applies to oppositely charged particles, while the particles with the same polarity of charge as the fibers are repelled before getting close. Particles can be charged by many natural factors such as cosmic rays, radiation, lightning, triboelectric charging via particle collision, etc.[25] Charge-neutral particles can be captured by electrostatic induction; i.e., they are polarized into dipoles by the electric field and thus become attracted to the fiber surface that has the largest electric field gradient. Both electrostatic filtration mechanisms work simultaneously with the aforementioned mechanical filtration mechanisms, and the amount that each contributes toward the total filtration efficiency depends on the particle size (Figure 2C). The particle size corresponding to the lowest filtration efficiency is termed the most penetrating particle size (MPPS), which is in the range of 0.1–0.3 μm for mechanical filtration mechanisms. However, the MPPS decreases with increasing fiber charge density[26] and is in the range of 30–60 nm for commercial electret filters,[27] such as many N95 masks.

In addition to the filtration efficiency, the pressure drop of a filter medium is another important parameter that determines the breathability of a mask. There is a trade-off between improving the filtration efficiency and decreasing the pressure drop. Therefore, the quality factor is usually used as the criterion for comparing different filter media. The quality factor is defined in Equation 1, where η is the filtration efficiency, and ΔP is the pressure drop:

$$\text{Quality factor} = -\frac{\ln(1-\eta)}{\Delta P}. \qquad \text{(Equation 1)}$$

Intrinsic Factors Affecting Filtration Performance

The thickness of a fibrous medium has the simplest relationship with its filtration performance. Increasing the thickness of a fibrous medium improves the filtration efficiency (i.e., decreases aerosol penetration) but also increases the pressure drop. The aerosol penetration $(1-\eta)$ decreases multiplicatively, and the pressure drop (ΔP) increases additively.[22] Therefore, according to Equation 1, the quality factor of a fibrous medium is independent of its thickness because the changes in the denominator and the numerator cancel out.[28]

The average fiber diameter of a fibrous medium significantly influences the filtration performance. Under the same packing density (i.e., the same porosity) and thickness, nanofibers provide a much higher surface area and a smaller pore size than microfibers (Figure 3A), both of which contribute to a higher filtration efficiency. In other words, a nanofiber medium can achieve the same filtration efficiency as a microfiber medium with much less material. On the other hand, decreasing the fiber diameter increases the pressure drop because the increased surface area leads to more air friction.[22,29] However, the effect of the fiber diameter on the quality factor (i.e., for a nanofiber medium and a microfiber medium of the same filtration efficiency, which one offers a lower pressure drop?) is still under debate in the literature: A simulation[26] based on the classic single-fiber model showed that decreasing the fiber diameter is detrimental to the quality factor for aerosol particles smaller than 0.1 μm; however, experimental studies[30] reported that decreasing the fiber diameter to the nanoscale (~100 nm) can actually improve the quality factor (Figure 3B). This contradiction stems from the assumption in the classic single-fiber model that the air velocity at the fiber surface is zero. This assumption breaks down when the fiber diameter is comparable with the mean free path of air molecules, which is 65 nm in ambient conditions. Thereby, the

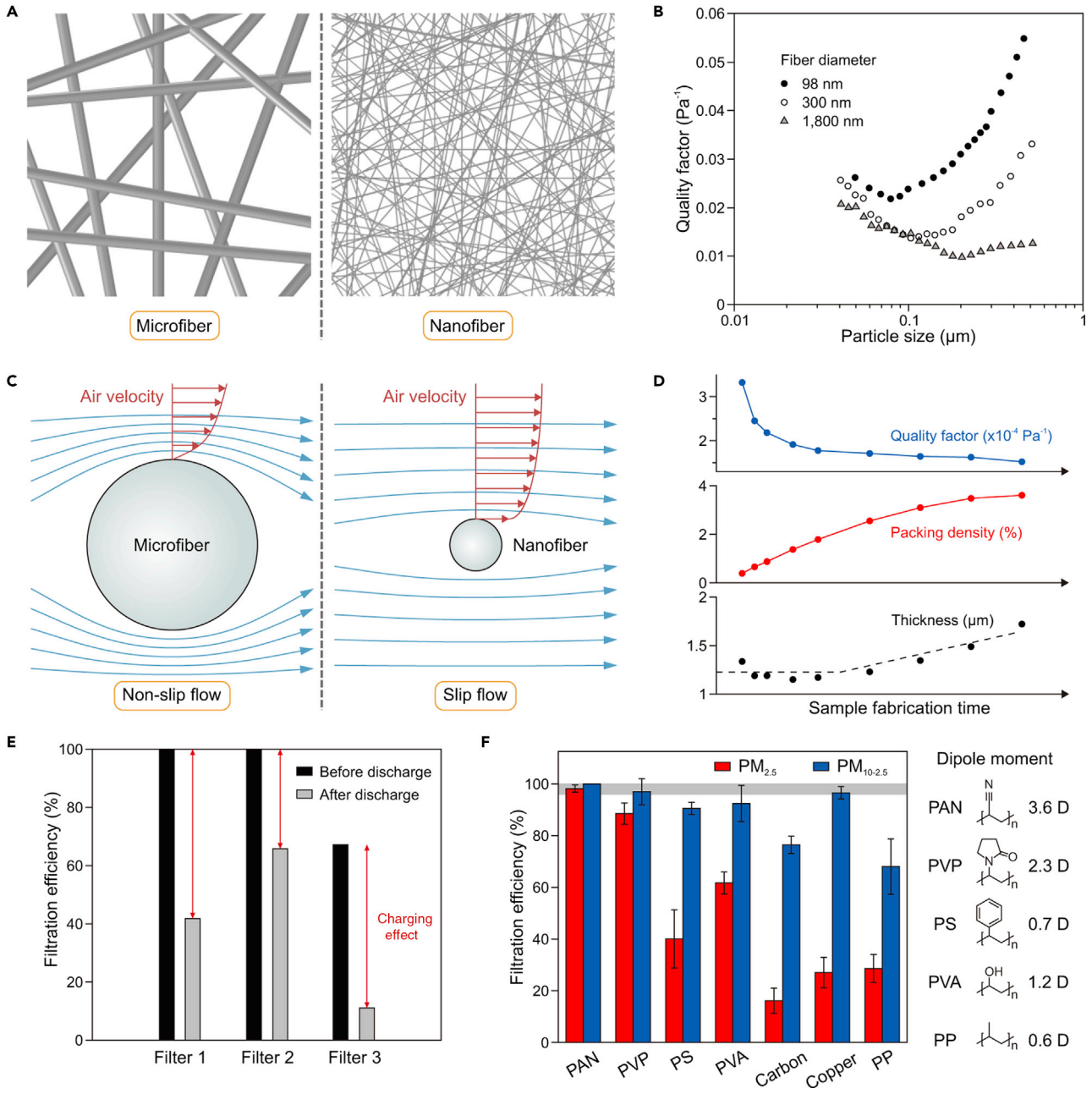

Figure 3. Intrinsic Factors Affecting Filtration Performance

(A) Schematic comparison of a microfiber medium (1-μm fiber diameter) and a nanofiber medium (100-nm fiber diameter) at the same packing density (2.5%).
(B) Quality factor of fibrous media with different average fiber diameters. Adapted from Leung et al.[30] with permission.
(C) Schematic illustration of the slip flow effect.
(D) Quality factor, packing density, and thickness of nanofiber media with different fabrication times (i.e., with different total mass of nanofibers per unit area). Adapted from Leung et al.[28] with permission.
(E) Filtration efficiency of three commercial electret filters, initially and after discharge in isopropyl alcohol. Adapted from Kilic et al.[24] with permission.
(F) Filtration efficiency of fibrous media made of different materials and the calculated dipole moment of the repeating unit of each polymer. All the samples have the same transmittance (~70%). Error bars, mean ± SD (n = 3). Adapted from Liu et al.[32] with permission.

slip flow effect must be taken into account for nanofibers[31] (Figure 3C) and has two beneficial effects: (1) there is less air drag on nanofibers than microfibers because fewer molecules exchange their momentum with the fibers, which translates into a lower pressure drop; (2) a larger proportion of air streamlines pass close to the surface of nanofibers than in the case of non-slip flow, resulting in a higher filtration efficiency via the interception mechanism.

The packing density, which is defined as the volume of the fibers divided by the total volume of the filter medium, is another

important geometric property that can affect the filtration performance. A higher packing density leads to less interstitial space and thus a higher filtration efficiency. However, an exceedingly high packing density leads to an extremely small pore size and thus an unpractical pressure drop.[22] For example, an expanded polytetrafluoroethylene membrane,[33] which has a much higher packing density than fibrous media, can provide a higher filtration efficiency at the cost of poor breathability, which limits its application in masks. The packing density is especially important for nanofiber media because the quality factor drops significantly as the packing density increases (blue and red curves in Figure 3D).[28] Furthermore, during the fabrication process of a nanofiber medium, the packing density first increases before the thickness starts to accumulate (red and green curves in Figure 3D).[28] Consequently, nanofiber media are usually used at very low packing density and small thickness to get a high quality factor, which in turn leads to two problems: (1) short service life and (2) mechanical fragility. The limited service life of a fibrous medium is because aerosol particles gradually accumulate on the fiber surface during filtration, causing clogging of the filter and resulting in a sharp increase in the pressure drop.[34] Leung et al.[35] reported that under continuous loading of submicrometer aerosols, the pressure drop of a nanofiber medium increases much faster than that of a microfiber medium. A solution to this is to put a microfiber medium upstream of the nanofiber medium, which prevents the nanofiber medium from clogging up too soon by filtering out larger particles and also provides mechanical support.[30]

Imparting electrostatic charge on a fibrous medium is one of the most effective ways to improve its quality factor because the electrostatic charge can enhance the filtration efficiency without increasing the pressure drop. A higher fiber charge density leads to a higher filtration efficiency.[26] These filters are called electret filters. Nearly all N95 masks on today's market are electret filters. The contribution of mechanical filtration mechanisms to the total filtration efficiency of an electret filter can be as low as 20%, depending on the size of the challenging particles, because electret filters are usually designed to have a more open structure than filters that rely solely on mechanical filtration mechanisms. As shown in Figure 3C, the filtration efficiency of three commercial electret filters decreases significantly after removing the electrostatic charge.[24] Therefore, the reliability of an electret filter depends on the stability of the electrostatic charge.

Unlike the geometric properties and charge density, the effect of the chemical composition (i.e., polymer species) of a fibrous medium on the filtration performance has been much less studied in the literature. The classic single-fiber model assumes a 100% adhesion efficiency, meaning that all the particles colliding with a fiber are captured. However, this is not true in reality because (1) a particle can bounce away when its impact velocity exceeds the critical sticking velocity,[36] or (2) a particle can slip around the surface of a fiber and then be released if the air drag force is higher than the friction force.[23] Therefore, a fibrous medium that has a stronger adhesive interaction with the aerosol particles provides a higher filtration efficiency. Liu et al.[32] compared the filtration efficiencies of fibrous media made of different polymers (Figure 3D) and found that the filtration efficiency increases with an increasing dipole moment of the polymer repeating units. They suggested that a dipole-dipole or induced-dipole force, which is the basis of most adhesion, enhanced the binding of the captured particles to the polymer surface.

Extrinsic Factors Affecting Filtration Performance

The face velocity, which is calculated as the volume flow rate divided by the area of a filter medium, is the most significant extrinsic factor that can have an impact on the filtration performance. A higher face velocity leads to a lower filtration efficiency and a higher pressure drop, both resulting in a lower quality factor. Therefore, increasing the area of a filter medium by pleating it in a confined space is a very effective way to improve the quality factor.[37] For example, a filtering facepiece respirator, such as an N95 mask, normally has a filtration area of about 180 cm^2. An elastomeric respirator normally has two cartridges with the filter medium pleated inside, resulting in a filtration area of about 400 cm^2 for the two cartridges. Therefore, an elastomeric respirator theoretically performs better yet is more expensive than a filtering facepiece, if the same filter medium is used. On the other hand, the volume flow rate of air exchanging through a mask can also directly affect the filtration efficiency. The inhalation flow rate of an adult ranges from 8 $L \cdot min^{-1}$ at rest to 120 $L \cdot min^{-1}$ during exercise. Instantaneous peak inhalation flow rates in the range of 300–400 $L \cdot min^{-1}$ were also recorded for certain activities that demand high workloads.[38] Eninger et al.[39] measured the aerosol penetration through an N95 mask under different inhalation flow rates (Figure 4A) and demonstrated that the N95 mask failed to maintain a minimum filtration efficiency of 95% under inhalation flow rates higher than 85 $L \cdot min^{-1}$. In addition, a high inhalation flow rate can lead to more aerosol particles penetrating through mask-face seal leakage.[40] Moreover, several studies[41,42] raised the concern that the test methods under constant air flow rates might overrate the filtration performance of a mask in actual pulsatile breathing conditions.

Humidity is another critical extrinsic factor that can affect the filtration performance, especially for electret filters. As discussed earlier, the filtration efficiency of an electret filter relies on its charge retention ability. However, the electrostatic charge of an electret filter inevitably decays in ambient conditions (Figure 4B).[43] Initially, the charges from shallow traps, such as the physical disorders originating from different polymer chain conformations,[45] are compensated by the intrinsic charge carriers, resulting in a rapid decay of the surface potential.[46] Afterward, the surface potential stabilizes because the remaining charge cannot escape from the deep traps, such as the chemical imperfections including double bond, hydroxyl, and carbonyl defects.[47] A higher humidity leads to more loss of the electrostatic charge and a shorter shelf life. This is because the absorbed water increases the electrical conductivity of the polymer fibers and thus facilitates the dissipation of the electrostatic charge.[44] Lee et al.[44] compared the charge decay phenomena of four electret filters made of different polymers and demonstrated that the extent of charge decay and performance reduction was directly proportional to the level of moisture regain after humidity aging (Figure 4C). Therefore, nonpolar polymers such as polyolefins are good candidates for making electret filters due to their high electrical resistivity and hydrophobicity, both of which are desirable for a better charge retention ability.

Sterilization methods that have minimum impact on the filtration performance are needed for the safe reuse of masks. This

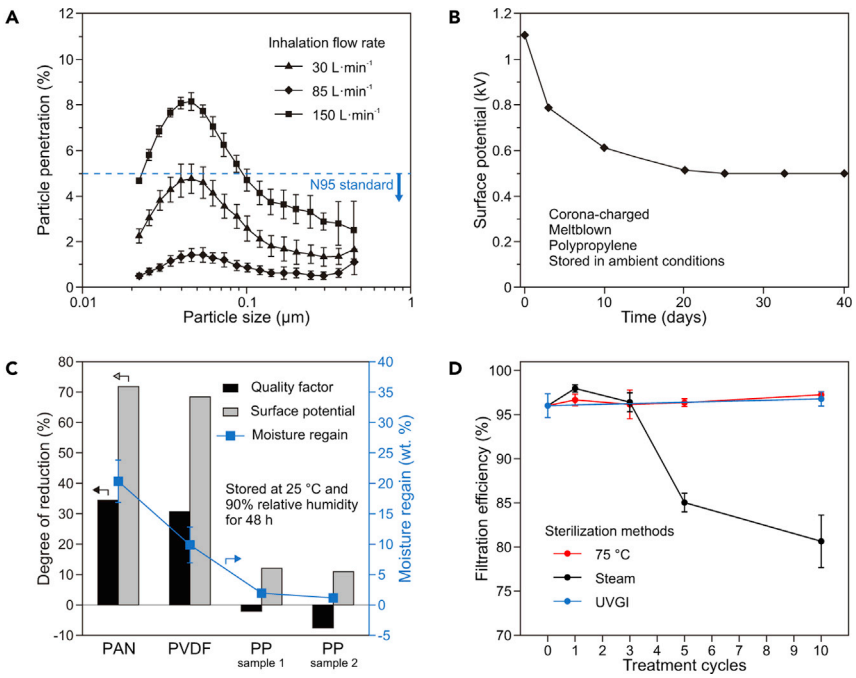

Figure 4. Extrinsic Factors Affecting Filtration Performance

(A) Percentage of particle penetration through an N95 mask under different inhalation flow rates. Error bars, mean ± SD (n = 3). Adapted from Eninger et al.[39] with permission.

(B) Decay of the electrostatic charge, reflected by the surface potential, of an electret filter in ambient conditions. Adapted from Motyl et al.[43] with permission.

(C) Reduction of the quality factor and the surface potential versus moisture regain of electret filters made of different polymers. Error bars, mean ± SD (n = 3). Adapted from Lee et al.,[44] CC BY 4.0.

(D) Change of the filtration efficiency of an N95 mask after cycles of sterilization treatment with different sterilization methods. Error bars, mean ± SD (n = 3). Adapted from Liao et al.[6] with permission.

becomes extremely important during a pandemic spread by the respiratory route, such as the ongoing COVID-19 pandemic, because health care workers often face shortages of N95 masks. Liao et al.[6] investigated the effects of five sterilization methods on the filtration efficiency of an N95 mask (Figure 4D), including (1) heat under various humidity levels, (2) steam, (3) 75% alcohol, (4) household diluted chlorine-based solution, and (5) ultraviolet germicidal irradiation (UVGI). They concluded that heat and UVGI are the best sterilization methods in terms of preserving the filtration performance. However, the sterilization efficiency of UVGI can be hampered by shadowing. Liao et al.[6] also advised against applying liquid, such as alcohol solutions, chlorine-based solutions, or soaps, to clean an N95 mask because this will lead to the dissipation of the electrostatic charge,[48] which is necessary for the mask to meet the N95 standard. Another promising way to sterilize N95 masks without sacrificing the filtration performance is fumigation with hydrogen peroxide;[49] however, this method requires special equipment that many hospitals do not possess.

FABRICATION OF FIBROUS MEDIA

Fibrous media can be fabricated by a wide variety of methods, such as airlaid, wetlaid, spunbond, meltblown, electrospinning, etc. Among these, meltblown and electrospinning are the most widely used techniques for making microfibers and nanofibers, respectively. The fabrics produced by other techniques have large average fiber diameter and thus poor filtration performance within a reasonable thickness. Therefore, meltblown and electrospinning are the main techniques for making filter media. In this section, we review the basic principles, the key processing parameters, and the recent development of meltblown and electrospinning. It is well known that the main disadvantages of electrospinning compared with meltblown are its low production rate and high cost. In view of this, we provide a discussion on the key challenges facing the industrial upscaling of electrospinning at the end of this section.

Meltblown

Meltblown is a cost-effective and high-throughput method to produce microfibers and is widely used in industry for manufacturing the filtration layers in masks.[50] Figure 5A illustrates a typical meltblown process: An extruder melts the polymer resin and delivers the melt to a die assembly, with a gear pump controlling the flow rate. At the tip of the die assembly, the melted polymer is extruded through small orifices and attenuated by the drag force of convergent streams of hot air. Turbulent air further fractures the polymer stream and creates microfibers, which begin to entangle. The entrainment of ambient air leads to fiber solidification as they fall toward the collector and form a self-bonded web. The die assembly is the most important part of a meltblown system and has been actively developed in the past decades (see Drabek et al.[51] for a recent review). Most commercial meltblown systems use a slot design[52] (Figure 5B), where numerous die orifices with a diameter of 0.2–0.6 mm are lined up at an interval of 10–20 orifices·cm^{-1}.

Polypropylene is by far the most popular polymer used in meltblown due to its high melt flow index (MFI), low melting point (160°C), low glass transition temperature (−10°C), low cost, and versatility in making a wide range of products. In principle, all thermoplastics can be meltblown, and indeed a wide variety of polymers (e.g., polyethylene, polystyrene, polyesters, polyamides, etc.) have been successfully demonstrated. However, the unsatisfactory rheological behaviors, especially the low MFI, of many polymers restrict them from forming a uniform web via meltblown.[55]

The average fiber diameter produced by commercial meltblown systems is, at best, in the range of 1–10 μm[56,57] (Figure 5C), and a typical attenuation ratio between the orifice diameter and the final fiber diameter is 100 (from 0.38 mm to 3.8 μm).[57] Six key processing parameters can affect the fiber diameter. (1) Increasing the air velocity decreases the fiber diameter by increasing the aerodynamic drag force;[58] however, a too high air velocity causes fiber breakage.[59] (2) Similarly, a lower

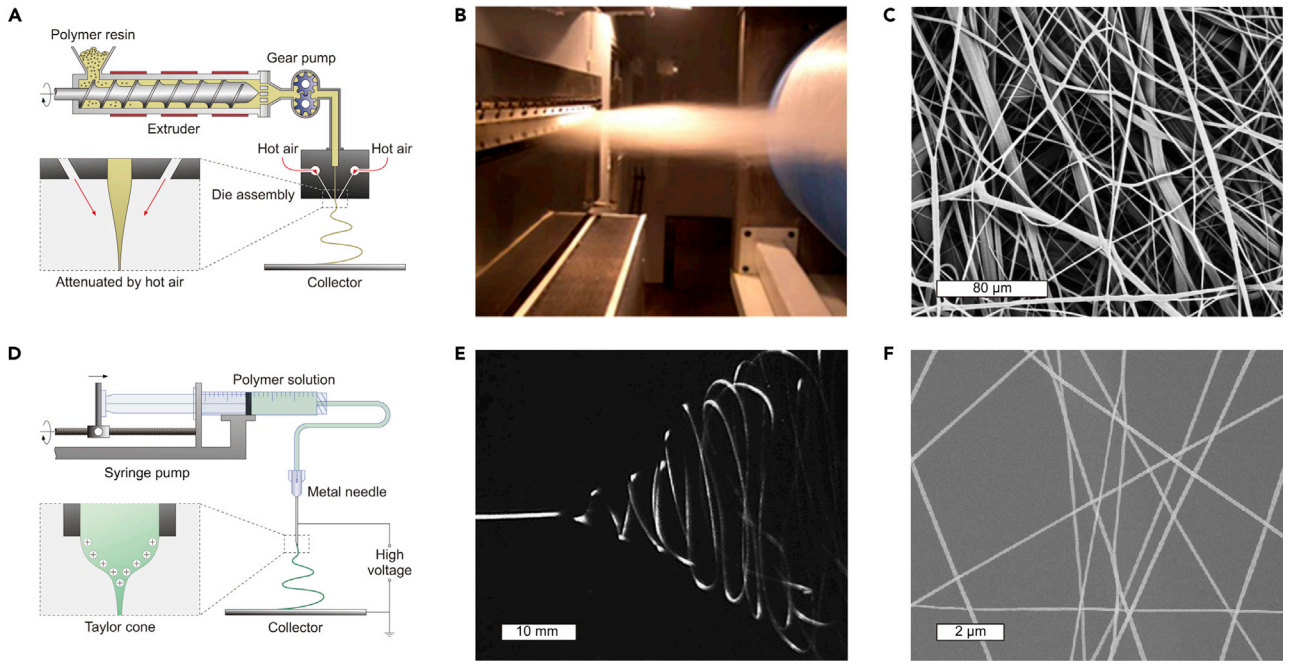

Figure 5. Fabrication of Fibrous Media

(A) Schematic illustration of meltblown.

(B) Photograph of a working slot die in a commercial meltblown system. Image courtesy of 4FFF, CC BY-SA 4.0, via Wikimedia Commons.

(C) SEM image of typical meltblown microfibers. Adapted from Liao et al.[6] with permission.

(D) Schematic illustration of electrospinning.

(E) Photograph of the whipping electrified jet in an electrospinning process. Adapted from Han et al.[53] with permission.

(F) SEM image of typical electrospun nanofibers. Adapted from Xu et al.[54] with permission.

polymer throughput decreases the fiber diameter because the same drag force is applied on less polymer mass.[60] (3) A higher MFI decreases the fiber diameter, and a common strategy to increase the MFI is to mix the polymer raw materials with a small amount of radical initiator, which induces thermomechanical degradation of the polymer along the extruder.[61] (4) A higher processing temperature decreases the fiber diameter by increasing the MFI as well as allowing additional attenuation before solidification, but the upper limit is prescribed by the degradation temperature of the polymer.[58] (5) A smaller orifice size reduces the fiber diameter, but an exceedingly small orifice leads to an uneconomical production rate, a high pressure needed to extrude the polymer, and a high probability of clogging by foreign particles present in the polymer feedstocks. (6) Increasing the die-to-collector distance decreases the fiber diameter but has little effect after exceeding a certain distance (~12 cm), because fiber attenuation occurs within a relatively short distance.[62,63]

Although there is a huge motivation to make finer meltblown fibers to achieve higher filtration efficiency, submicrometer-diameter meltblown fibers have only been reported on a laboratory scale. For example, Ellison et al.[64] achieved an average fiber diameter of 300 nm by carefully modifying the processing parameters (lowering the throughput, increasing the processing temperature, and increasing the air velocity) on a conventional 0.2-mm single-orifice die. Hassan et al.[65] reported the design of a die with 0.127-mm orifices, which could produce polypropylene fibers with an average diameter of 330 nm at a production rate of 2.23 $kg \cdot h^{-1}$ per meter of die width. Pu et al.[66] introduced a static electric field into a commercial meltblown apparatus and reduced the average fiber diameter from 1.69 μm to 0.96 μm. Soltani et al.[67] achieved a record low average fiber diameter of 36 nm based on a new concept of the islands-in-the-sea meltblown process (an immiscible polymer blend was meltblown, and nanofibers were obtained by extracting the sacrificial polymer matrix with an appropriate solvent), but the nanofibers tended to bundle together and were too dense for use in air filtration.

Electrospinning

Electrospinning is a simple and versatile tool to fabricate nanofibers and has attracted increasing attention from academia for its application in air filtration.[68] Figure 5D illustrates the basic setup for electrospinning: A polymer solution is hosted in a syringe and fed through a metal needle, with a syringe pump controlling the flow rate. A high voltage (1–30 kV) is applied between the needle and a grounded collector, which is placed 10–20 cm away. At the tip of the needle, a pendent droplet of the polymer solution, held by its surface tension, is charged and elongated into a conical shape (known as the Taylor cone). Once the intensity of the electric field surpasses a threshold, the Coulombic force exerted by the electric field together with the electrostatic repulsion between the surface charges overcome the surface tension and force the ejection of an electrified jet from the tip of the Taylor cone. The electrified jet then undergoes a whipping process[53] (Figure 5E) with the solvent evaporated, leading to the formation of a charged polymer fiber, which is randomly deposited on the grounded collector.

A wide variety of polymers have been successfully electrospun into nanofibers (see Huang et al.[69] for a comprehensive list). Polyacrylonitrile (using dimethylformamide as the solvent) and nylon (using formic acid as the solvent) are two commonly used polymers in air filtration research. However, electrospinning polyolefins, such as polypropylene and polyethylene, is challenging because they can only be dissolved in nonpolar solvents, and the corresponding polymer solutions cannot build up sufficient surface charge for the Taylor cone to form.[70] Although melt electrospinning has emerged as a promising alternative, the diameter of the resulting fibers is generally larger than 1 μm.[71]

The biggest advantage of electrospinning compared with meltblown is that 100-nm-diameter fibers can be easily produced (Figure 5F). During the whipping process, the electrified jet attenuates as much as three orders of magnitude from the Taylor cone to the final fiber.[72] Electrospun nanofibers with a diameter less than 10 nm were also reported.[73,74] Three key processing parameters can affect the fiber diameter. (1) Decreasing the viscosity of the precursor solution can reduce the fiber diameter. This can be achieved by decreasing the polymer concentration, using polymers with lower molecular weight, or raising the processing temperature.[75] (2) Increasing the conductivity of the precursor solution decreases the fiber diameter because a higher charge density strengthens the electrostatic repulsion, leading to a smaller Taylor cone and enhanced stretch during the whipping process.[76] Adding salt is a common strategy to increase the solution conductivity.[77] (3) A stronger electric field reduces the fiber diameter by exerting a stronger electrostatic force.[78] This can be achieved by increasing the working voltage or decreasing the needle-to-collector distance. An often encountered problem in electrospinning is the formation of beads along the as-spun fibers or even the breakup of the electrified jet into droplets, which is usually caused by an insufficient solution viscosity or an exceedingly high electric field.[79] An excessive solution feed rate can also lead to beaded fibers.[80]

The main disadvantages of electrospinning compared with meltblown are its low production rate and high cost. This is mainly due to four reasons. (1) Although a straightforward way to increase the throughput is to increase the number of needles, a primary challenge stems from the deterioration of the local electric field at the needle tip due to the presence of neighboring needles.[81] Theron et al.[82] demonstrated that an inter-needle distance larger than 1 cm is necessary for process stability and the uniformity of the as-spun fibrous medium. In comparison, the interval between the die orifices in meltblown is normally less than 1 mm. (2) Another challenge for high-throughput production is polymer clogging in needles, especially when a high-volatility solvent is used.[83] In this respect, needleless electrospinning, featuring the formation of multiple electrified jets directly from an open liquid surface, possesses higher scaling-up potential. A wide variety of spinnerets have been developed (see Niu et al.[84] for a recent review). However, because the jet initiation in needleless electrospinning is a self-organized process, the spinning process is hard to control, resulting in a wide distribution of fiber diameter and limited configurability (e.g., impracticality of core-shell fiber structures, etc.). (3) The use of a volatile organic solvent in electrospinning accounts for its higher cost compared with that of meltblown. The solvent takes up more than 80 wt % of the precursor solution and is usually more expensive than the dissolved polymer. Moreover, without proper treatment or recovery, the evaporated solvent poses a hazard to the operators and the environment. Although many solvent-free electrospinning methods have been developed (see Zhang et al.[85] for a recent review), only microfibers were successfully spun due to the high viscosity and low conductivity of the precursor liquids. (4) Another limitation of electrospinning is that the fiber collector must be conductive, whereas meltblown can lay fibers directly on a non-conductive fabric. Varesano et al.[86] showed that using a spunbond nonwoven fabric instead of an aluminum foil as the substrate results in a much lower production rate and sometimes even failure to produce uniform fibers. This is because the deposited charged fibers are not able to discharge themselves and will repel the incoming fibers by Coulombic force. A promising solution is electrospinning on a conductive substrate that has minimum adhesion to the spun fibers (e.g., copper foil with surface microstructure), followed by peeling off the nanofiber medium and transferring it to a desired substrate.[54]

ELECTROSTATIC CHARGING

As discussed earlier, imparting electrostatic charge on a fibrous medium is the most effective way to improve its filtration performance. An electrostatically charged filter medium is also called an electret filter. Electrostatic charging has been widely used in fabricating masks. Nearly all of the N95 masks on today's market are electrostatically charged. In this section, we first review the mechanisms and recent developments of two major electrostatic charging methods used in industry: corona discharge and triboelectric charging. We then discuss the residual charge in electrospun nanofibers, with a focus on its decay behavior. We end this section with a review on recent efforts using nanoparticle additives as charge enhancers, which we envision as a promising direction worth further exploration.

Corona Discharge

Corona discharge is the most popular method in industry for making electret filters due to the speed of charging and the simplicity of the setup. A corona discharge is the ionization of the gas molecules between a pair of electrodes under a sufficiently high potential difference. The output current is limited to prevent electrical breakdown or arcing. The pair of electrodes usually have asymmetric shapes, such as a biased fine wire above a grounded roller (Figure 6A).[87] A fibrous medium can be charged as it travels through the gap between the two electrodes. Ions form near the emitting electrode, drift under the electric field, and then deposit on the surface of the fibers. Over time, the surface charges can move into the bulk and be trapped at depths of several micrometers, which is dependent on the material properties. Other electrode configurations[88] were also invented to be used at different stages[89] of the meltblown process. For example, a patent by Moosmayer et al.[90] applied corona discharge directly on the molten fibers before the web formation by putting two biased wire electrodes at the exit of a grounded slot die (Figure 6B). A patent by Deeds[91] applied corona discharge upstream of the hot air pathway, and the ionized molecules were blown out by the hot air to charge

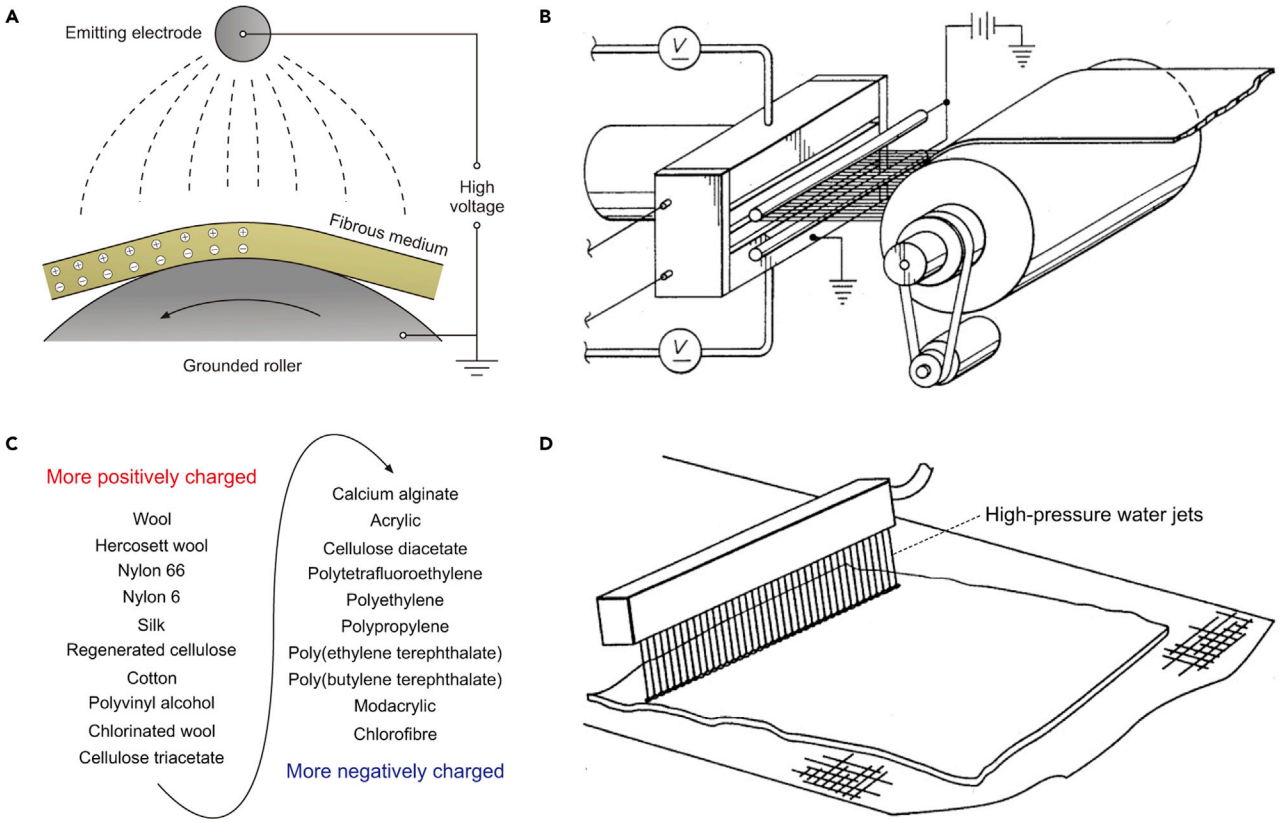

Figure 6. Conventional Methods for Making Electret Filters

(A) Schematic illustration of a typical electrode configuration for corona discharge: a biased wire above a grounded roller. A fibrous medium is charged as it travels through the gap.

(B) Schematic illustration of an electrode configuration for corona discharge, which is integrated with a meltblown process: two biased wire electrodes at the exit of a grounded slot die. Adapted from Moosmayer et al.[90]

(C) Triboelectric series of textile yarns. Adapted from Smith et al.[92] with permission.

(D) Schematic illustration of hydro-charging, which utilizes the triboelectric effect between water and polymers. Adapted from Angadjivand et al.[93]

the molten fibers. An ionic hairdryer can also be used to charge a mask via a similar mechanism.

Three key processing parameters can affect the stability and the density of the imparted charges. (1) A positive bias rather than a negative bias is usually used because the latter leads to more surface oxidation,[94] resulting in a higher moisture regain and a faster charge decay.[95] (2) A higher electric field leads to a higher charge density, which can be achieved by increasing the potential on the emitting electrode or decreasing the distance between the electrodes. However, an exceedingly high electric field generates sparks and causes pinholes in the fibrous medium,[96] which is detrimental to the filtration efficiency. (3) Prolonging the charging duration can also enhance the charge density, yet the imparted charge reaches saturation within a couple of minutes.[97]

Triboelectric Charging

Triboelectric charging is another way to make electret filters, which relies on the spontaneous charge exchange between dissimilar materials on contact.[92] The farther away two materials are from each other on the triboelectric series (Figure 6C), the greater the charge exchange. The earliest electret filter (the Hansen filter) was made by triboelectric charging: wool fibers and resin particles were rubbed together via the carding process and then needle-punched to produce the filter medium, where the wool fibers were positively charged and the resin particles were negatively charges. A modern development uses a blend of polypropylene fibers and modacrylic fibers, where the polypropylene fibers are positively charged and the modacrylic fibers are negatively charged. Tsai et al.[98] compared triboelectric charging with corona discharge and showed that triboelectric charging provided a higher charge density and a higher filtration efficiency. However, conventional triboelectric charging is incompatible with meltblown or electrospinning, because it relies on the carding process and thus cannot be directly applied on an as-formed fibrous medium. Hydro-charging was later invented to solve this problem by utilizing the triboelectric effect between water and polymers.[93] Specifically, high-pressure water jets are impinged onto a fibrous medium (Figure 6D), which is further dried at increased temperature to imbue an electrostatic charge.

There are also some recent research efforts on utilizing the triboelectric effect for making electret filters. For example, Gu et al.[99] used a rotating triboelectric nanogenerator (R-TENG) to charge a filter medium made of electrospun polyamide acid nanofibers on a metallic grid (Figure 7A). The rotator of the R-TENG was driven by an electric motor, and the output voltage

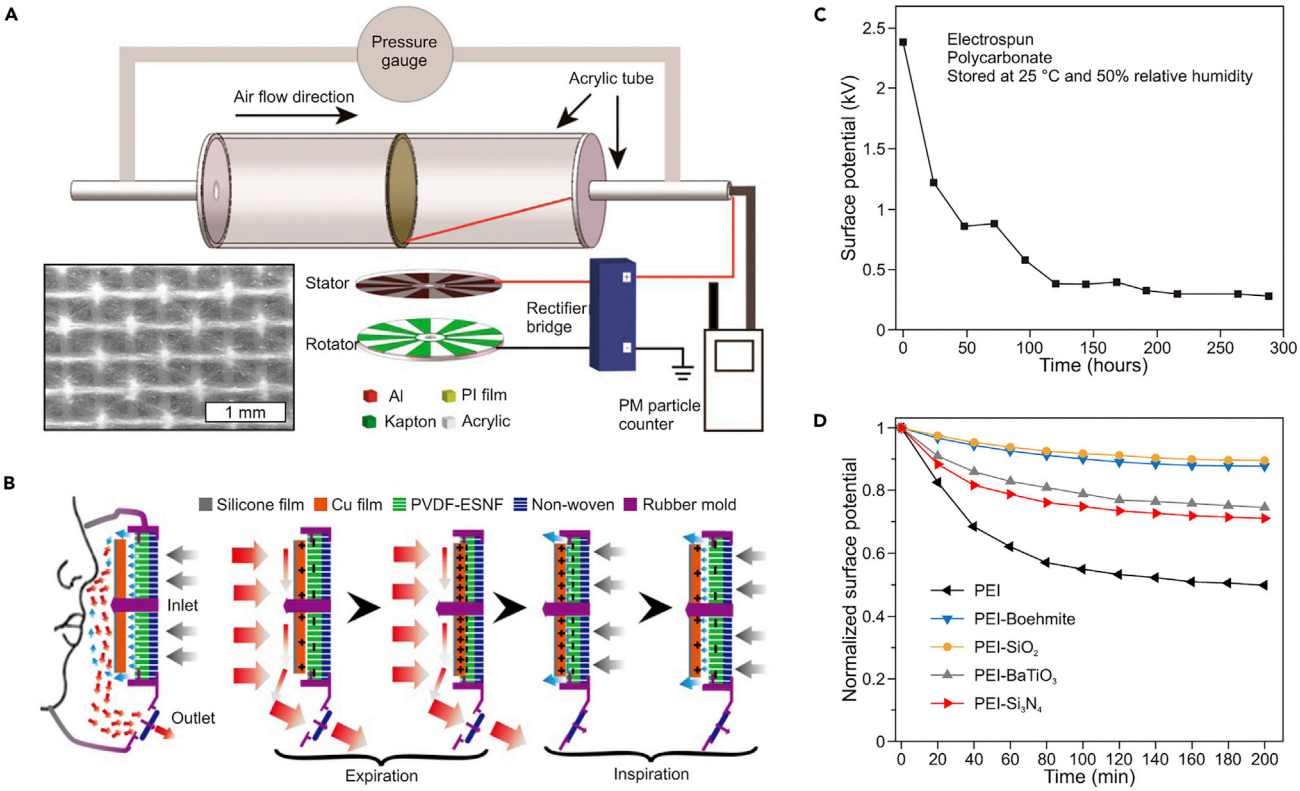

Figure 7. Recent Development in Making Electret Filters

(A) Filter medium charged by an R-TENG. The working mechanism of the R-TENG relies on the triboelectric effect. Adapted from Gu et al.[99] with permission.

(B) Working principle of a self-charged mask. The filter medium, which was made of electrospun polyvinylidene fluoride nanofibers (PVDF-ESNF), was charged by the contact electrification with a copper foil under the periodic force exerted by the air flow of breathing. Adapted from Liu et al.[100] with permission.

(C) Decay of the residual charge, reflected by the surface potential, in electrospun polycarbonate nanofibers at 25°C and 50% relative humidity. Adapted from Cho et al.[103] with permission.

(D) Decay of the residual charge, reflected by the normalized surface potential, in electrospun polyetherimide (PEI) nanofibers doped with different electret nanoparticles. Adapted from Li et al.[104] with permission.

was rectified into a constant-polarity voltage (~480 V) and then applied to the metallic grid. Such design required external energy input for the electric motor. The same group later reported a self-charged version,[100] as shown in Figure 7B. The filter medium made of electrospun polyvinylidene fluoride nanofibers was charged by contact electrification with a copper foil. The repeating contact and separation between the fibrous medium and the copper foil was driven by the periodic force exerted by the airflow of breathing. Bai et al.[101] reported a washable filter medium made of a woven polytetrafluoroethylene fabric and a woven nylon fabric. The filter medium can be charged after washing by rubbing the two fabrics against each other. Han et al.[102] showed that a filter medium made of electrospun poly(vinylidene fluoride-co-trifluoroethylene) nanofibers can be triboelectrically charged by brushing with a microfiber nylon duster. A common limitation of the above works is that only the surface of the filter media can be charged.

Residual Charge in Electrospun Nanofibers

Electrospinning is often considered a good method for making electret filters because of the presence of residual charges in electrospun nanofibers, meaning that fabricating a fibrous medium and electrostatically charging it can be integrated into a single step.[105] However, the ability of electrospun nanofiber to retain the residual charge is usually unsatisfactory.[98] This is because: (1) only polar polymers can be electrospun into nanofibers; although melt electrospinning is applicable to nonpolar polymers, the diameter of the resulting fibers is generally larger than 1 μm;[71] (2) fibrous media made of polar polymers are more prone to losing the electrostatic charge in humid air than those made of nonpolar polymers.[44]

Many past studies have investigated the decay of the residual charge in electrospun nanofibers. For example, Cho et al.[103] showed that the surface potential of an electrospun polycarbonate sample decayed from 2,400 V to 400 V (83% decay) after 125 h of storage at 25°C and 50% relative humidity (Figure 7C). Schreuder-Gibson et al.[106] demonstrated that the surface potential of an electrospun polyacrylonitrile sample decayed from 1,950 V to 214 V (89% decay) after 3 months of storage in ambient conditions, and that of an electrospun polystyrene sample decayed from −3,332 V to −40 V (99% decay) under the same conditions. In comparison, the surface potential of a corona-charged meltblown polypropylene sample decayed from 1,100 V to 500 V (55% decay) after 40 days of storage in ambient conditions (Figure 4B).[43] These comparisons point out that the initial surface potential of fibrous media made of polar

Box 1. Open Questions Remaining to Be Resolved

1. **How will the chemical properties of aerosol particles affect the filtration efficiency?** Most previous experimental studies used NaCl aerosol or dioctyl phthalate aerosol as the challenging agent for testing filtration efficiency. However, the chemical composition of the aerosols in real scenarios are much more complicated, especially considering the wide variety of emission sources of $PM_{2.5}$.[114] Understanding the contribution of the chemical interactions between the aerosol particles and the fibers toward the filtration efficiency is of practical significance.
2. **How to design and fabricate a nanofiber-microfiber composite filter for improving the quality factor?** As discussed in the text (Figure 3D), a nanofiber medium offers a higher quality factor at a lower packing density; however, it is challenging to fabricate a thick (thick enough for an acceptable filtration efficiency) nanofiber medium with a low packing density because, during electrospinning, nanofibers tend to collapse into a thinner and more packed morphology due to their poor mechanical strength. A promising solution is to alternately arrange thin and low-packing-density nanofiber layers and microfiber layers into a composite filter. Although similar concepts have been demonstrated in the literature,[30,115] questions such as how to tune the thickness ratio between each layer to maximize the quality factor and how to fabricate such composite filters at low cost still need to be answered.
3. **What is the spatial distribution of the captured particles in a fibrous medium?** We envision that a clear 3D image of the captured particle distribution through the thickness of a fibrous medium will provide vital insights into the filtration mechanism (e.g., to see if there are regions that capture notably more particles than other regions). X-ray computed tomography and cross-sectional electron microscopy might be appropriate tools to achieve this.
4. **What is the spatial distribution of the electrostatic charge in an electret fibrous medium?** Electrostatic voltmeters and electrostatic field meters are the two most commonly used tools described in the literature for characterizing the electrostatic charge. However, they can only measure the surface potential, which can be converted to the surface charge density; they fail to elucidate the charge density in the bulk of an electret fibrous medium. Further development of characterizing techniques with improved spatial resolution in 3D will enable us to resolve this question and motivate more advancements in electret filters.

polymers by electrospinning is usually higher yet decays faster than that of corona-charged polypropylene fibrous media. Such difference is not only caused by the charging methods. Polyolefins such as polypropylene intrinsically have a better charge retention ability than polar polymers due to their higher electrical resistivity and hydrophobicity, as discussed in earlier (Figure 4C).

Nanoparticle Additives as Charge Enhancers

As discussed earlier, the charge retention ability of an electret filter is important for its long-term reliability. A promising way to improve the charge retention ability is to incorporate electret nanoparticles into the fibers of a fibrous medium, which can be achieved by mixing the nanoparticles with the precursor solution for electrospinning or with the polymer resins for meltblown. Many different electret nanoparticles have been investigated, including boehmite,[107] $BaTiO_3$,[108,109] SiO_2,[104] TiO_2,[110] tourmaline,[111] etc. Li et al.[104] compared the effects of adding different electret nanoparticles on the charge retention ability of electrospun polyetherimide nanofibers and found that SiO_2 and boehmite were the most effective (Figure 7D). Although most past studies attributed the enhanced charge storage ability to the stable dipole orientation in the electret nanoparticles formed during the charging process, a scientifically proven mechanism is still lacking. Particularly, a theory that can explain the different degrees of enhancement of different nanoparticle additives is needed for future development.

In addition to inorganic nanoparticles, particles made of organic compounds can also be used as charge enhancers. Wang et al.[112] reported that incorporating 0.05 wt % polytetrafluoroethylene nanoparticles effectively improved the stability and the density of the residual charge in electrospun polyvinylidene fluoride nanofibers. They explained that the additional charge storage capacity originated from the interfacial polarization between the two polymers during the electrospinning process. Xiao et al.[113] demonstrated that adding stearate or rosin improved the filtration efficiency and the storage stability of a corona-charged meltblown polypropylene fibrous medium. They found that with the presence of stearate or rosin during the meltblown process, the crystallinity of the resulting polypropylene fibers increased, and the crystallite size decreased. They thereby inferred that adding stearate or rosin resulted in more interfaces between the crystallite and the amorphous regions, which contributed to the enhanced charge storage capacity.

OUTLOOK ON FUTURE DIRECTIONS

In countries such as China and Japan, masks are societal norms that serve as the first line of defense against $PM_{2.5}$ pollution and pathogen transmission; however, in the wake of the COVID-19 pandemic, masks have become the "new normal" in many parts of the world. With a sudden increase in demand, a resurgence of interest is expected for the research and development of masks. On the one hand, improving the filtration performance and reducing the manufacturing cost will remain the main focus of research in this field, and several open questions are still to be answered, which are summarized in Box 1. On the other hand, new research opportunities will arise in response to the unprecedented changes brought on by the COVID-19 pandemic. The results of these findings could also lead to better protection against $PM_{2.5}$ air pollution. In this section, we highlight four research directions that are most needed and promising from our perspective.

First, conferring masks with biocidal properties will further decrease the risk of pathogen transmission. A recent study[116]

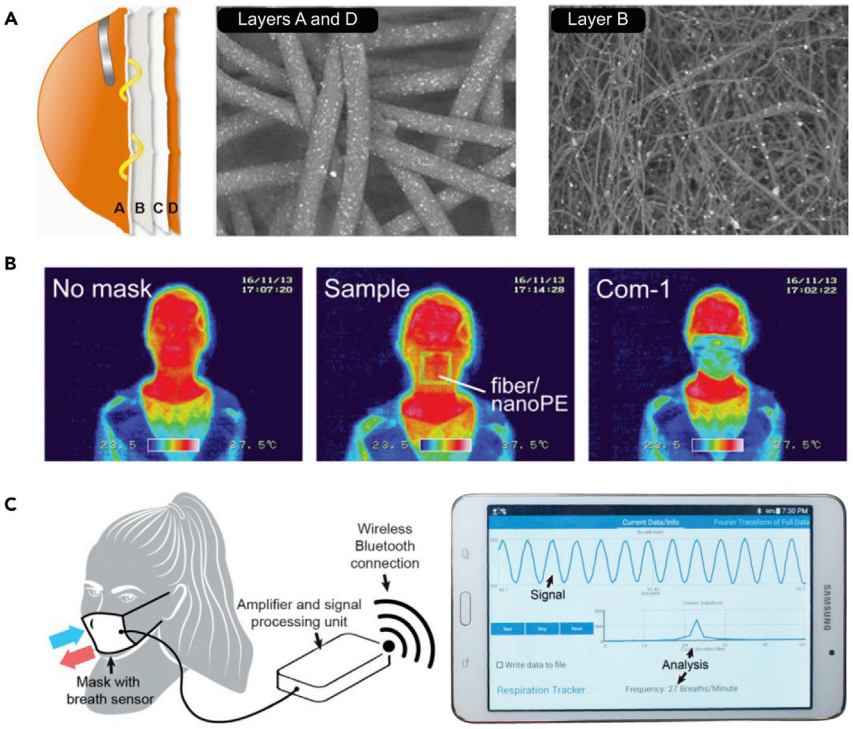

Figure 8. Research Opportunities Amid the COVID-19 Pandemic

(A) Schematic illustration of an antiviral mask, which is composed of two external spunbond polypropylene layers (layers A and D) containing 2.2 wt % copper oxide particles, one internal meltblown polypropylene layer (layer B) containing 2 wt % copper oxide particles, and one mechanically supportive layer made of plain polyester. Adapted from Borkow et al.,[121] CC BY 4.0.

(B) Thermal imaging of a bare face (left panel), a face covered with a radiative-cooling mask (middle panel), and a face covered with a commercial mask (right panel) demonstrating that the radiative-cooling mask is transparent to mid-infrared light. Adapted from Yang et al.[128] with permission.

(C) Schematic illustration of a mask for respiration monitoring with the embedded moisture sensor and electronics (left panel). Photograph of a tablet computer running an Android app that can display and analyze the incoming data stream from the data acquisition electronics (right panel). Adapted from Güder et al.[129] with permission.

revealed that 72 h are required for the SARS-CoV-1 and SARS-CoV-2 viruses on plastic surfaces to be reduced by three orders of magnitude. Assuming a similar longevity on mask surfaces, improper use and disposal of masks could increase the risk of pathogen transmission rather than reducing it. In addition, the particles captured on mask surfaces can be re-aerosolized during exhalation and may still be infectious, especially when the wearer sneezes or coughs.[117] There have been many studies on incorporating different biocidal additives into the fibers of filter media, such as silver,[118–120] copper oxide,[121] N-halamines,[122,123] quaternary ammonium salts,[124] and herbal extracts.[125–127] However, most studies only investigated the antibacterial properties, and limited studies[121,126] evaluated the effectiveness of the additives in deactivating pathogenic viruses. For example, Borkow et al.[121] demonstrated that impregnation of CuO nanoparticles endowed masks with antiviral properties against the human influenza A virus (H1N1) and the avian influenza virus (H9N2) (Figure 8A). More research is needed to determine the antiviral potency of other biocidal additives, especially against the SARS-CoV-2 virus, as well as their impact on the filtration performance.

Second, improving the thermal comfort of masks will greatly benefit the health care workers fighting the pandemic and increase the public acceptance of wearing masks, especially in warmer and higher humidity environments. Exhalation valves were designed to improve thermal comfort by allowing unfiltered exhaled breath to flow out quickly, yet pathogens can also escape through the valves and potentially infect others. The US Centers for Disease Control and Prevention recommends hospitals not use masks with exhalation valves where a sterile field must be maintained,[130] and wearing such masks does not comply with the mask mandates currently enacted in many US states.[131] Therefore, another heat dissipation mechanism is needed to prevent the uncomfortable buildup of heat inside masks. Radiation plays an indispensable role in the dissipation of human body heat; mid-infrared light can be emitted by human skin in the form of black body radiation (7–14 μm with an output peak at 9.5 μm).[132] The concept of a radiative-cooling textile was first demonstrated by Hsu et al.[133] in 2016 based on a nanoporous polyethylene membrane. Yang et al.[128] later introduced this concept into masks by integrating electrospun nylon-6 nanofibers with a needle-punched nanoporous polyethylene membrane (Figure 8B). There is still a lot to improve following this route, and a recent review by Peng et al.[134] serves as a good foundation for future development.

Third, as masks become part of our daily lives, they also provide an emerging wearable platform for integrating functional electronics, especially sensors to record health-related data. One promising direction is to monitor respiration rate, which is an important metric for predicting cardiac arrest,[135] diagnosing sleep apnea,[136] and determining the anaerobic threshold during exercise.[137] Güder et al.[129] demonstrated a mask that could monitor respiration rate with a paper-based moisture sensor attached inside (Figure 8C). The moisture sensor converted the changes in humidity caused by cycles of inhalation and exhalation into electrical signals. Several other studies demonstrated similar concepts with different moisture-sensitive materials, including graphene oxide,[138] alginate,[139] and polydopamine.[140] Aside from monitoring respiration rate, in the literature, we found that other functions, such as the detection of formaldehyde and ammonia in the air,[141] were also integrated into masks, yet the purpose of these functions in masks was not well justified. Nevertheless, with the study by Güder et al.[129] as an encouraging example, we envision that smart masks represent a promising direction for the development of wearable electronics.

Fourth, the increased popularity of wearing masks will bring significant environmental impacts. The manufacturing of masks generates considerable environmental footprints and

greenhouse gas emissions. For example, the volatile organic solvent used in electrospinning is usually toxic and could pose a hazard to the environment without proper treatment. Therefore, developing solvent-free electrospinning[85] is important for enhancing the sustainability of this manufacturing process. On the other hand, disposed masks contain contaminated waste and can lead to plastic waste on both land and in the ocean.[142,143] Thus, it is imperative to conduct research on discovering eco-friendly mask materials and exploring effective reuse and waste management systems to minimize the environmental impacts. A wide variety of biodegradable polymers, such as cellulose, starch, chitin, chitosan, etc., have been successfully electrospun into nanofibers, providing a promising path toward eco-friendly masks;[144] nevertheless, more research is needed to determine the filtration efficiency of fibrous media made of these biodegradable polymers, especially after long-term storage in different humidity levels.

Considering that $PM_{2.5}$ pollution will continue to be a major health concern in newly industrialized countries, and the current pandemic may create lasting cultural shifts in many parts of the world to increase mask usage, the pursuit of more efficient and cost-effective masks will be a cornerstone to maintaining public health. Just as masks are desperately needed for this ongoing fight against COVID-19, further development of masks is essential in the fight against $PM_{2.5}$ pollution and future global health emergencies. We hope this article helps researchers gain a comprehensive picture of the historic and current development of masks and motivates more technological advancements in the near future.

ACKNOWLEDGMENTS

Y.C. acknowledges support from the United States Department of Energy (DOE) Office of Science through the National Virtual Biotechnology Laboratory, a consortium of DOE national laboratories focused on response to COVID-19, with funding provided by the Coronavirus CARES Act. J.X. acknowledges Haimeng Zhang for helpful discussion.

AUTHOR CONTRIBUTIONS

J.X. and Y.C. conceived the outline. J.X. wrote the manuscript. X.X. and R.X. helped write the section on outlook on future directions. W.Z. helped write the section on factors affecting filtration performance. S.C.K. helped write the section on fabrication of fibrous media. Y.C. helped write the section on filtration mechanisms. T.T.H. helped write the section on electrostatic charging. E.W. helped write the Introduction.

REFERENCES

1. Burnett, R., Chen, H., Szyszkowicz, M., Fann, N., Hubbell, B., Pope, C.A., Apte, J.S., Brauer, M., Cohen, A., Weichenthal, S., et al. (2018). Global estimates of mortality associated with long-term exposure to outdoor fine particulate matter. Proc. Natl. Acad. Sci. U S A *115*, 9592–9597.
2. Mahowald, N. (2011). Aerosol indirect effect on biogeochemical cycles and climate. Science *334*, 794–796.
3. Horton, D.E., Skinner, C.B., Singh, D., and Diffenbaugh, N.S. (2014). Occurrence and persistence of future atmospheric stagnation events. Nat. Clim. Change *4*, 698–703.
4. Pope, C.A., Burnett, R.T., Turner, M.C., Cohen, A., Krewski, D., Jerrett, M., Gapstur, S.M., and Thun, M.J. (2011). Lung cancer and cardiovascular disease mortality associated with ambient air pollution and cigarette smoke: shape of the exposure–response relationships. Environ. Health Perspect. *119*, 1616–1621.
5. Ritchie, H., and Roser, M. (2019). Outdoor Air Pollution. Our World in Data. https://ourworldindata.org/outdoor-air-pollution#share-exposed-to-air-pollution-above-who-limits.
6. Liao, L., Xiao, W., Zhao, M., Yu, X., Wang, H., Wang, Q., Chu, S., and Cui, Y. (2020). Can N95 respirators be reused after disinfection? How many times? ACS Nano *14*, 6348–6356.
7. Dong, E., Du, H., and Gardner, L. (2020). An interactive web-based dashboard to track COVID-19 in real time. Lancet Infect. Dis. *20*, 533–534.
8. World Health Organization. (2020). Modes of transmission of virus causing COVID-19: implications for IPC precaution recommendations. https://www.who.int/news-room/commentaries/detail/modes-of-transmission-of-virus-causing-covid-19-implications-for-ipc-precaution-recommendations.
9. Kutter, J.S., Spronken, M.I., Fraaij, P.L., Fouchier, R.A., and Herfst, S. (2018). Transmission routes of respiratory viruses among humans. Curr. Opin. Virol. *28*, 142–151.
10. Lewis, S. (2020). "An Open License to Pollute": Trump Administration Indefinitely Suspends Some Environmental Protection Laws during Coronavirus Pandemic (CBS NEWS). https://www.cbsnews.com/news/coronavirus-trump-administration-epa-suspends-environmental-protection-laws.
11. Xu, M., and Goh, B. (2020). China to Modify Environmental Supervision of Firms to Boost Post-coronavirus Recovery (Reuters). https://ca.reuters.com/article/instant-article/idUSKBN20X0AG.
12. McNeill, V.F. (2020). COVID-19 and the air we breathe. ACS Earth Space Chem. *4*, 674–675.
13. Zhu, Y., Xie, J., Huang, F., and Cao, L. (2020). Association between short-term exposure to air pollution and COVID-19 infection: evidence from China. Sci. Total Environ. *727*, 138704.
14. Zhang, Z., Xue, T., and Jin, X. (2020). Effects of meteorological conditions and air pollution on COVID-19 transmission: evidence from 219 Chinese cities. Sci. Total Environ. *741*, 140244.
15. Comunian, S., Dongo, D., Milani, C., and Palestini, P. (2020). Air pollution and COVID-19: the role of particulate matter in the spread and increase of COVID-19's morbidity and mortality. Int. J. Env Res. Pub He *17*, 4487.
16. Wang, B., Chen, H., Chan, Y.L., and Oliver, B.G. (2020). Is there an association between the level of ambient air pollution and COVID-19? Am. J. Physiol. Lung Cell Mol. Physiol. *319*, L416–L421.
17. Zhao, M., Liao, L., Xiao, W., Yu, X., Wang, H., Wang, Q., Lin, Y.L., Kilinc-Balci, F.S., Price, A., Chu, L., et al. (2020). Household materials selection for homemade cloth face coverings and their filtration efficiency enhancement with triboelectric charging. Nano Lett. *20*, 5544–5552.
18. Konda, A., Prakash, A., Moss, G.A., Schmoldt, M., Grant, G.D., and Guha, S. (2020). Aerosol filtration efficiency of common fabrics used in respiratory cloth masks. ACS Nano *14*, 6339–6347.
19. Ptak, T.J. (2017). Gas filtration. In Fibrous Filter Media, P. Brown and C. Cox, eds. (Elsevier), pp. 3–26.
20. Mukhopadhyay, A. (2014). Composite nonwovens in filters: theory. In Composite Non-woven Materials, D. Das and B. Pourdeyhimi, eds. (Elsevier), pp. 120–163.
21. Lee, K.W., and Liu, B.Y.H. (1982). Theoretical study of aerosol filtration by fibrous filters. Aerosol Sci. Technol. *1*, 147–161.
22. Wang, X., Kim, K., Lee, C., and Kim, J. (2008). Prediction of air filter efficiency and pressure drop in air filtration media using a stochastic simulation. Fibers Polym. *9*, 34–38.
23. Sambaer, W., Zatloukal, M., and Kimmer, D. (2011). 3D modeling of filtration process via polyurethane nanofiber based nonwoven filters prepared by electrospinning process. Chem. Eng. Sci. *66*, 613–623.
24. Kilic, A., Russell, S., Shim, E., and Pourdeyhimi, B. (2017). The charging and stability of electret filters. In Fibrous Filter Media, P. Brown and C. Cox, eds. (Elsevier), pp. 95–121.
25. Zhang, L., Gu, Z., Yu, C., Zhang, Y., and Cheng, Y. (2016). Surface charges on aerosol particles – accelerating particle growth rate and atmospheric pollution. Indoor Built Environ. *25*, 437–440.
26. Huang, S.-H., Chen, C.-W., Kuo, Y.-M., Lai, C.-Y., McKay, R., and Chen, C.-C. (2013). Factors affecting filter penetration and quality factor of particulate respirators. Aerosol Air Qual. Res. *13*, 162–171.
27. Rengasamy, S., Eimer, B.C., and Shaffer, R.E. (2009). Comparison of nanoparticle filtration performance of NIOSH-approved and CE-marked particulate filtering facepiece respirators. Ann. Occup. Hyg. *53*, 117–128.
28. Leung, W.W.-F., Hung, C.-H., and Yuen, P.-T. (2010). Effect of face velocity, nanofiber packing density and thickness on filtration performance of filters with nanofibers coated on a substrate. Separat. Purif. Technol. *71*, 30–37.

29. Hung, C.-H., and Leung, W.W.-F. (2011). Filtration of nano-aerosol using nanofiber filter under low Peclet number and transitional flow regime. Separat. Purif. Technol. *79*, 34–42.
30. Leung, W.W.-F., and Hung, C.-H. (2012). Skin effect in nanofiber filtration of submicron aerosols. Separat. Purif. Technol. *92*, 174–180.
31. Li, P., Wang, C., Zhang, Y., and Wei, F. (2014). Air filtration in the free molecular flow regime: a review of high-efficiency particulate air filters based on carbon nanotubes. Small *10*, 4543–4561.
32. Liu, C., Hsu, P.-C., Lee, H.-W., Ye, M., Zheng, G., Liu, N., Li, W., and Cui, Y. (2015). Transparent air filter for high-efficiency PM2.5 capture. Nat. Commun. *6*, 1–9.
33. Wikol, M., Hartmann, B., Brendle, J., Crane, M., Beuscher, U., Brake, J., and Shickel, T. (2019). Expanded polytetrafluoroethylene membranes and their applications. In Filtration and Purification in the Biopharmaceutical Industry, M. Jornitz and T. Meltzer, eds. (CRC Press), pp. 619–640.
34. Thomas, D., Penicot, P., Contal, P., Leclerc, D., and Vendel, J. (2001). Clogging of fibrous filters by solid aerosol particles Experimental and modelling study. Chem. Eng. Sci. *56*, 3549–3561.
35. Leung, W.W.-F., and Hung, C.-H. (2008). Investigation on pressure drop evolution of fibrous filter operating in aerodynamic slip regime under continuous loading of sub-micron aerosols. Separat. Purif. Technol. *63*, 691–700.
36. Wang, H.-C., and Kasper, G. (1991). Filtration efficiency of nanometer-size aerosol particles. J. Aerosol Sci. *22*, 31–41.
37. Chen, C.W., Huang, S.H., Chiang, C.M., Hsiao, T.C., and Chen, C.C. (2008). Filter quality of pleated filter cartridges. Ann. Occup. Hyg. *52*, 207–212.
38. Caretti, D.M., Gardner, P.D., and Coyne, K.M. (2004). Workplace Breathing Rates: Defining Anticipated Values and Ranges for Respirator Certification Testing (US Army Research, Development, and Engineering Command), Report ECBC-TR-316.
39. Eninger, R.M., Honda, T., Adhikari, A., Heinonen-Tanski, H., Reponen, T., and Grinshpun, S.A. (2008). Filter performance of N99 and N95 facepiece respirators against viruses and ultrafine particles. Ann. Occup. Hyg. *52*, 385–396.
40. Rengasamy, S., and Eimer, B.C. (2012). Nanoparticle penetration through filter media and leakage through face seal interface of N95 filtering facepiece respirators. Ann. Occup. Hyg. *56*, 568–580.
41. Grinshpun, S.A., Haruta, H., Eninger, R.M., Reponen, T., McKay, R.T., and Lee, S.-A. (2009). Performance of an N95 filtering facepiece particulate respirator and a surgical mask during human breathing: two pathways for particle penetration. J. Occup. Environ. Hyg. *6*, 593–603.
42. Eshbaugh, J.P., Gardner, P.D., Richardson, A.W., and Hofacre, K.C. (2008). N95 and P100 respirator filter efficiency under high constant and cyclic flow. J. Occup. Environ. Hyg. *6*, 52–61.
43. Motyl, E., and Łowkis, B. (2006). Effect of air humidity on charge decay and lifetime of PP electret nonwovens. Fibers Textiles East. Europe *14*, 39–42.
44. Lee, J., and Kim, J. (2020). Material properties influencing the charge decay of electret filters and their impact on filtration performance. Polymers *12*, 721.
45. Teyssedre, G., and Laurent, C. (2005). Charge transport modeling in insulating polymers: from molecular to macroscopic scale. IEEE Trans. Dielect. Electr. Insul. *12*, 857–875.
46. Małecki, J.A. (1999). Linear decay of charge in electrets. Phys. Rev. B *59*, 9954–9960.
47. Stournara, M.E., and Ramprasad, R. (2010). A first principles investigation of isotactic polypropylene. J. Mater. Sci. *45*, 443–447.
48. Xiao, H., Song, Y., and Chen, G. (2014). Correlation between charge decay and solvent effect for melt-blown polypropylene electret filter fabrics. J. Electrostatics *72*, 311–314.
49. Schwartz, A., Stiegel, M., Greeson, N., Vogel, A., Thomann, W., Brown, M., Sempowski, G.D., Alderman, T.S., Condreay, J.P., Burch, J., et al. (2020). Decontamination and reuse of N95 respirators with hydrogen peroxide vapor to address worldwide personal protective equipment shortages during the SARS-CoV-2 (COVID-19) pandemic. Appl. Biosaf *25*, 67–70.
50. Dutton, K. (2008). Overview and analysis of the meltblown process and parameters. J. Textile Apparel *6*, 1–24.
51. Drabek, J., and Zatloukal, M. (2019). Meltblown technology for production of polymeric microfibers/nanofibers: a review. Phys. Fluids *31*, 091301.
52. Zhao, R. (2002). Melt blown dies: a hot innovation spot. Int. Nonwovens J. *11*, 37–41.
53. Han, T., Reneker, D.H., and Yarin, A.L. (2007). Buckling of jets in electrospinning. Polymer *48*, 6064–6076.
54. Xu, J., Liu, C., Hsu, P.-C., Liu, K., Zhang, R., Liu, Y., and Cui, Y. (2016). Roll-to-roll transfer of electrospun nanofiber film for high-efficiency transparent air filter. Nano Lett. *16*, 1270–1275.
55. Müller, D.H., and Krobjilowski, A. (2001). Meltblown fabrics from biodegradable polymers. Int. Nonwovens J. *10*, 11–17.
56. Han, W., Wang, X., and Bhat, G. (2013). Structure and air permeability of melt blown nanofiber webs. J. Nanomater. Mol. Nanotechnol. *2*, 1–5.
57. Moore, E.M., Papavassiliou, D.V., and Shambaugh, R.L. (2004). Air velocity, air temperature, fiber vibration and fiber diameter measurements on a practical melt blowing die. Int. Nonwovens J. *13*, 43–53.
58. Bresee, R.R., and Qureshi, U.A. (2006). Influence of process conditions on melt blown web structure. Part IV—fiber diameter. J. Engineered Fibers Fabrics *1*, 32–46.
59. Bresee, R.R., and Qureshi, U.A. (2002). Fiber motion near the collector during melt blowing. Part 2—fly formation. Int. Nonwovens J. *11*, 21–27.
60. Chen, T., Li, L., and Huang, X. (2005). Fiber diameter of polybutylene terephthalate melt-blown nonwovens. J. Appl. Polym. Sci. *97*, 1750–1752.
61. Machado, A.V., Maia, J.M., Canevarolo, S.V., and Covas, J.A. (2004). Evolution of peroxide-induced thermomechanical degradation of polypropylene along the extruder. J. Appl. Polym. Sci. *91*, 2711–2720.
62. Yin, H., Yan, Z., Ko, W.-C., and Bresee, R.R. (2000). Fundamental description of the melt blowing process. Int. Nonwovens J. *9*, 25–28.
63. Uppal, R., Bhat, G., Eash, C., and Akato, K. (2013). Meltblown nanofiber media for enhanced quality factor. Fibers Polym. *14*, 660–668.
64. Ellison, C.J., Phatak, A., Giles, D.W., Macosko, C.W., and Bates, F.S. (2007). Melt blown nanofibers: fiber diameter distributions and onset of fiber breakup. Polymer *48*, 3306–3316.
65. Hassan, M.A., Yeom, B.Y., Wilkie, A., Pourdeyhimi, B., and Khan, S.A. (2013). Fabrication of nanofiber meltblown membranes and their filtration properties. J. Membr. Sci. *427*, 336–344.
66. Pu, Y., Zheng, J., Chen, F., Long, Y., Wu, H., Li, Q., Yu, S., Wang, X., and Ning, X. (2018). Preparation of polypropylene micro and nanofibers by electrostatic-assisted melt blown and their application. Polymers *10*, 959.
67. Soltani, I., and Macosko, C.W. (2018). Influence of rheology and surface properties on morphology of nanofibers derived from islands-in-the-sea meltblown nonwovens. Polymer *145*, 21–30.
68. Zhu, M., Han, J., Wang, F., Shao, W., Xiong, R., Zhang, Q., Pan, H., Yang, Y., Samal, S.K., Zhang, F., et al. (2017). Electrospun nanofibers membranes for effective air filtration. Macromol. Mater. Eng. *302*, 1600353.
69. Huang, Z.-M., Zhang, Y.-Z., Kotaki, M., and Ramakrishna, S. (2003). A review on polymer nanofibers by electrospinning and their applications in nanocomposites. Composites Sci. Technol. *63*, 2223–2253.
70. Angammana, C.J., and Jayaram, S.H. (2011). Analysis of the effects of solution conductivity on electrospinning process and fiber morphology. IEEE Trans. Ind. Applicat. *47*, 1109–1117.
71. Brown, T.D., Dalton, P.D., and Hutmacher, D.W. (2016). Melt electrospinning today: an opportune time for an emerging polymer process. Prog. Polym. Sci. *56*, 116–166.
72. Fridrikh, S.V., Yu, J.H., Brenner, M.P., and Rutledge, G.C. (2003). Controlling the fiber diameter during electrospinning. Phys. Rev. Lett. *90*, 144502.
73. Hou, H., Jun, Z., Reuning, A., Schaper, A., Wendorff, J.H., and Greiner, A. (2002). Poly(p-xylylene) nanotubes by coating and removal of ultrathin polymer template fibers. Macromolecules *35*, 2429–2431.
74. Huang, C., Chen, S., Lai, C., Reneker, D.H., Qiu, H., Ye, Y., and Hou, H. (2006). Electrospun polymer nanofibres with small diameters. Nanotechnology *17*, 1558–1563.
75. Mit-uppatham, C., Nithitanakul, M., and Supaphol, P. (2004). Ultrafine electrospun polyamide-6 fibers: effect of solution conditions on morphology and average fiber diameter. Macromol. Chem. Phys. *205*, 2327–2338.
76. Uyar, T., and Besenbacher, F. (2008). Electrospinning of uniform polystyrene fibers: the effect of solvent conductivity. Polymer *49*, 5336–5343.
77. Balgis, R., Kartikowati, C.W., Ogi, T., Gradon, L., Bao, L., Seki, K., and Okuyama, K. (2015). Synthesis and evaluation of straight and bead-free nanofibers for improved aerosol filtration. Chem. Eng. Sci. *137*, 947–954.
78. Yang, Y., Jia, Z., Liu, J., Li, Q., Hou, L., Wang, L., and Guan, Z. (2008). Effect of electric field distribution uniformity on electrospinning. J. Appl. Phys. *103*, 104307.
79. Liu, Y., He, J.-H., Yu, J., and Zeng, H. (2008). Controlling numbers and sizes of beads in electrospun nanofibers. Polym. Int. *57*, 632–636.

80. Zargham, S., Bazgir, S., Tavakoli, A., Rashidi, A.S., and Damerchely, R. (2012). The effect of flow rate on morphology and deposition area of electrospun nylon 6 nanofiber. J. Engineered Fibers Fabrics *7*, https://doi.org/10.1177/155892501200700414.

81. Angammana, C.J., and Jayaram, S.H. (2011). The effects of electric field on the multijet electrospinning process and fiber morphology. IEEE Trans. Ind. Applicat. *47*, 1028–1035.

82. Theron, S.A., Yarin, A.L., Zussman, E., and Kroll, E. (2005). Multiple jets in electrospinning: experiment and modeling. Polymer *46*, 2889–2899.

83. Kanjanapongkul, K., Wongsasulak, S., and Yoovidhya, T. (2010). Prediction of clogging time during electrospinning of zein solution: scaling analysis and experimental verification. Chem. Eng. Sci. *65*, 5217–5225.

84. Niu, H., and Lin, T. (2012). Fiber generators in needleless electrospinning. J. Nanomater. *2012*, 1–13.

85. Zhang, B., Yan, X., He, H.-W., Yu, M., Ning, X., and Long, Y.-Z. (2017). Solvent-free electrospinning: opportunities and challenges. Polym. Chem. *8*, 333–352.

86. Varesano, A., Rombaldoni, F., Mazzuchetti, G., Tonin, C., and Comotto, R. (2010). Multi-jet nozzle electrospinning on textile substrates: observations on process and nanofibre mat deposition. Polym. Int. *59*, 1606–1615.

87. Tsai, P.P., and Wadsworth L.C. (1995). Method and apparatus for the electrostatic charging of a web or film. US patent 5401446, filed October 9, 1992, and granted March 28, 1995.

88. Tsai, P.P., Qin, G., and Wadsworth, L.C. (1998). Theory and techniques of electrostatic charging of melt-blown nonwoven webs. Tappi J. *81*, 274–278.

89. Tsai, P.P., Qin, G., and Hassenboehler, C. (2000). Comparison of electrostatic charging at different locations in the melt blowing process. Int. Nonwovens J. *9*, 8–14.

90. Moosmayer, P., Budliger, J.P., Zurcher, E., and Wadsworth, L.C. (1990). Apparatus for electrically charging meltblown webs. US patent 4904174, filed September 15, 1988, and granted February 27, 1990.

91. Deeds, W.E. (1992). Charging apparatus and method for meltblown webs. US patent 5122048, filed September 24, 1990, and granted June 16, 1992.

92. Smith, P.A., East, G.C., Brown, R.C., and Wake, D. (1988). Generation of triboelectric charge in textile fibre mixtures, and their use as air filters. J. Electrostatics *21*, 81–98.

93. Angadjivand, S.A., Jones, M.E., and Meyer, D.E. (1996). Method of charging electret filter media. US patent 5496507, filed August 17, 1994, and granted March 5, 1996.

94. Yovcheva, T.A., Avramova, I.A., Mekishev, G.A., and Marinova, T.S. (2007). Corona-charged polypropylene electrets analyzed by XPS. J. Electrostatics *65*, 667–671.

95. Wang, X., Zhang, X., Pan, D., Cao, G., and Xia, Z. (2009). Charge storage capability of cross-linked polypropylene electret films. 2009 IEEE 9th International Conference on the Properties and Applications of Dielectric Materials (IEEE), pp. 926–929.

96. Das, D., Thakur, R., and Pradhan, A.K. (2012). Optimization of corona discharge process using Box–Behnken design of experiments. J. Electrostatics *70*, 469–473.

97. Plopeanu, M.-C., Dascalescu, L., Yahiaoui, B., Antoniu, A., Hulea, M., and Notingher, P.V. (2011). Distribution of electric potential at the surface of corona-charged non-woven fabrics. 2011 IEEE Industry Applications Society Annual Meeting (IEEE), pp. 1–5.

98. Tsai, P.P., Schreuder-Gibson, H., and Gibson, P. (2002). Different electrostatic methods for making electret filters. J. Electrostatics *54*, 333–341.

99. Gu, G.Q., Han, C.B., Lu, C.X., He, C., Jiang, T., Gao, Z.L., Li, C.J., and Wang, Z.L. (2017). Triboelectric nanogenerator enhanced nanofiber air filters for efficient particulate matter removal. ACS Nano *11*, 6211–6217.

100. Liu, G., Nie, J., Han, C., Jiang, T., Yang, Z., Pang, Y., Xu, L., Guo, T., Bu, T., Zhang, C., et al. (2018). Self-powered electrostatic adsorption face mask based on a triboelectric nanogenerator. ACS Appl. Mater. Interfaces *10*, 7126–7133.

101. Bai, Y., Han, C.B., He, C., Gu, G.Q., Nie, J.H., Shao, J.J., Xiao, T.X., Deng, C.R., and Wang, Z.L. (2018). Washable multilayer triboelectric air filter for efficient particulate matter $PM_{2.5}$ removal. Adv. Funct. Mater. *28*, 1706680.

102. Han, K.S., Lee, S., Kim, M., Park, P., Lee, M.H., and Nah, J. (2019). Electrically activated ultrathin PVDF-TrFE air filter for high-efficiency $PM_{1.0}$ filtration. Adv. Funct. Mater. *29*, 1903633.

103. Cho, B.M., Nam, Y.S., Cheon, J.Y., and Park, W.H. (2015). Residual charge and filtration efficiency of polycarbonate fibrous membranes prepared by electrospinning. J. Appl. Polym. Sci. *132*, https://doi.org/10.1002/app.41340.

104. Li, X., Wang, N., Fan, G., Yu, J., Gao, J., Sun, G., and Ding, B. (2015). Electreted polyetherimide–silica fibrous membranes for enhanced filtration of fine particles. J. Colloid Interfaces Sci. *439*, 12–20.

105. Catalani, L.H., Collins, G., and Jaffe, M. (2007). Evidence for molecular orientation and residual charge in the electrospinning of poly(butylene terephthalate) nanofibers. Macromolecules *40*, 1693–1697.

106. Schreuder-Gibson, H.L., Gibson, P., and Tsai, P. (2004). Cooperative charging effects of fibers from electrospinning of electrically dissimilar polymers. Int. Nonwovens J. *13*, 39–45.

107. Yeom, B.Y., Shim, E., and Pourdeyhimi, B. (2010). Boehmite nanoparticles incorporated electrospun nylon-6 nanofiber web for new electret filter media. Macromol. Res. *18*, 884–890.

108. Kilic, A., Shim, E., and Pourdeyhimi, B. (2015). Electrostatic capture efficiency enhancement of polypropylene electret filters with barium titanate. Aerosol Sci. Technol. *49*, 666–673.

109. Wang, N., Cai, M., Yang, X., and Yang, Y. (2018). Electret nanofibrous membrane with enhanced filtration performance and wearing comfortability for face mask. J. Colloid Interf. Sci. *530*, 695–703.

110. Cho, D., Naydich, A., Frey, M.W., and Joo, Y.L. (2013). Further improvement of air filtration efficiency of cellulose filters coated with nanofibers via inclusion of electrostatically active nanoparticles. Polymer *54*, 2364–2372.

111. Yu, B., Han, J., Sun, H., Zhu, F., Zhang, Q., and Kong, J. (2015). The preparation and property of poly(lactic acid)/tourmaline blends and melt-blown nonwoven. Polym. Compos. *36*, 264–271.

112. Wang, S., Zhao, X., Yin, X., Yu, J., and Ding, B. (2016). Electret polyvinylidene fluoride nanofibers hybridized by polytetrafluoroethylene nanoparticles for high-efficiency air filtration. ACS Appl. Mater. Interfaces *8*, 23985–23994.

113. Xiao, H., Gui, J., Chen, G., and Xiao, C. (2015). Study on correlation of filtration performance and charge behavior and crystalline structure for melt-blown polypropylene electret fabrics. J. Appl. Polym. Sci. *132*, 42807.

114. Zhang, R., Liu, C., Zhou, G., Sun, J., Liu, N., Hsu, P.-C., Wang, H., Qiu, Y., Zhao, J., Wu, T., et al. (2018). Morphology and property investigation of primary particulate matter particles from different sources. Nano Res. *11*, 3182–3192.

115. Leung, W.W.-F., Hau, C.W.-Y., and Choy, H.-F. (2018). Microfiber-nanofiber composite filter for high-efficiency and low pressure drop under nano-aerosol loading. Separat. Purif. Technol. *206*, 26–38.

116. van Doremalen, N., Bushmaker, T., Morris, D.H., Holbrook, M.G., Gamble, A., Williamson, B.N., Tamin, A., Harcourt, J.L., Thornburg, N.J., Gerber, S.I., et al. (2020). Aerosol and surface stability of SARS-CoV-2 as compared with SARS-CoV-1. N. Engl. J. Med. *382*, 1564–1567.

117. Qian, Y., Willeke, K., Grinshpun, S.A., and Donnelly, J. (1997). Performance of N95 respirators: reaerosolization of bacteria and solid particles. Am. Ind. Hyg. Assoc. J. *58*, 876–880.

118. Zhang, L., Luo, J., Menkhaus, T.J., Varadaraju, H., Sun, Y., and Fong, H. (2011). Antimicrobial nano-fibrous membranes developed from electrospun polyacrylonitrile nanofibers. J. Membr. Sci. *369*, 499–505.

119. Jung, J.H., Hwang, G.B., Lee, J.E., and Bae, G.N. (2011). Preparation of airborne Ag/CNT hybrid nanoparticles using an aerosol process and their application to antimicrobial air filtration. Langmuir *27*, 10256–10264.

120. Wang, C., Wu, S., Jian, M., Xie, J., Xu, L., Yang, X., Zheng, Q., and Zhang, Y. (2016). Silk nanofibers as high efficient and lightweight air filter. Nano Res. *9*, 2590–2597.

121. Borkow, G., Zhou, S.S., Page, T., and Gabbay, J. (2010). A novel anti-influenza copper oxide containing respiratory face mask. PLoS One *5*, e11295.

122. Demir, B., Cerkez, I., Worley, S.D., Broughton, R.M., and Huang, T.-S. (2015). N-Halamine-modified antimicrobial polypropylene nonwoven fabrics for use against airborne bacteria. ACS Appl. Mater. Interfaces *7*, 1752–1757.

123. Huang, C., Liu, Y., Li, Z., Li, R., Ren, X., and Huang, T.-S. (2019). N-halamine antibacterial nanofibrous mats based on polyacrylonitrile and N-halamine for protective face masks. J. Engineered Fibers Fabrics *14*, 1–8.

124. Nicosia, A., Gieparda, W., Foksowicz-Flaczyk, J., Walentowska, J., Wesołek, D., Vazquez, B., Prodi, F., and Belosi, F. (2015). Air filtration and antimicrobial capabilities of electrospun PLA/PHB containing ionic liquid. Separat. Purif. Technol. *154*, 154–160.

125. Huang, R., Pyankov, O.V., Yu, B., and Agranovski, I.E. (2010). Inactivation of fungal spores collected on fibrous filters by *Melaleuca alternifolia* (tea tree oil). Aerosol Sci. Technol. *44*, 262–268.

126. Pyankov, O.V., Usachev, E.V., Pyankova, O., and Agranovski, I.E. (2012). Inactivation of airborne influenza virus by tea tree and Eucalyptus oils. Aerosol Sci. Technol. *46*, 1295–1302.

127. Choi, J., Yang, B.J., Bae, G.-N., and Jung, J.H. (2015). Herbal extract incorporated nanofiber fabricated by an electrospinning technique and its application to antimicrobial air filtration. ACS Appl. Mater. Interfaces *7*, 25313–25320.

128. Yang, A., Cai, L., Zhang, R., Wang, J., Hsu, P.-C., Wang, H., Zhou, G., Xu, J., and Cui, Y. (2017). Thermal management in nanofiber-based face mask. Nano Lett. *17*, 3506–3510.

129. Güder, F., Ainla, A., Redston, J., Mosadegh, B., Glavan, A., Martin, T.J., and Whitesides, G.M. (2016). Paper-based electrical respiration sensor. Angew. Chem. Int. Ed. *55*, 5727–5732.

130. US Centers for Disease Control (2020). Prevention Personal Protective Equipment: Questions and Answers. https://www.cdc.gov/coronavirus/2019-ncov/hcp/respirator-use-faq.html.

131. Webeck, E. (2020). Coronavirus: Bay Area mask order takes effect Wednesday. Here's what You Need to Know. The Mercury News https://www.mercurynews.com/2020/04/22/coronavirus-bay-area-mask-order-takes-effect-wednesday-heres-what-you-need-to-know.

132. Hardy, J.D., and DuBois, E.F. (1937). Regulation of heat loss from the human body. Proc. Natl. Acad. Sci. U S A *23*, 624–631.

133. Hsu, P.-C., Song, A.Y., Catrysse, P.B., Liu, C., Peng, Y., Xie, J., Fan, S., and Cui, Y. (2016). Radiative human body cooling by nanoporous polyethylene textile. Science *353*, 1019–1023.

134. Peng, Y., and Cui, Y. (2020). Advanced textiles for personal thermal management and energy. Joule *4*, 724–742.

135. Fieselmann, J.F., Hendryx, M.S., Helms, C.M., and Wakefield, D.S. (1993). Respiratory rate predicts cardiopulmonary arrest for internal medicine inpatients. J. Gen. Intern. Med. *8*, 354–360.

136. Peppard, P.E., Young, T., Barnet, J.H., Palta, M., Hagen, E.W., and Hla, K.M. (2013). Increased prevalence of sleep-disordered breathing in adults. Am. J. Epidemiol. *177*, 1006–1014.

137. Carey, D.G., Schwarz, L.A., Pliego, G.J., and Raymond, R.L. (2005). Respiratory rate is a valid and reliable marker for the anaerobic threshold: implications for measuring change in fitness. J. Sports Sci. Med. *4*, 482–488.

138. Li, B., Xiao, G., Liu, F., Qiao, Y., Li, C.M., and Lu, Z. (2018). A flexible humidity sensor based on silk fabrics for human respiration monitoring. J. Mater. Chem. C *6*, 4549–4554.

139. Zhang, J., Wang, X.-X., Zhang, B., Ramakrishna, S., Yu, M., Ma, J.-W., and Long, Y.-Z. (2018). In situ assembly of well-dispersed Ag nanoparticles throughout electrospun alginate nanofibers for monitoring human breath—smart fabrics. ACS Appl. Mater. Interfaces *10*, 19863–19870.

140. Chen, L., Huang, Y., Song, L., Yin, W., Hou, L., Liu, X., and Chen, T. (2019). Biofriendly and regenerable emotional monitor from interfacial ultrathin 2D PDA/AuNPs cross-linking films. ACS Appl. Mater. Interfaces *11*, 36259–36269.

141. Gao, Z., Lou, Z., Chen, S., Li, L., Jiang, K., Fu, Z., Han, W., and Shen, G. (2018). Fiber gas sensor-integrated smart face mask for room-temperature distinguishing of target gases. Nano Res. *11*, 511–519.

142. Aragaw, T.A. (2020). Surgical face masks as a potential source for microplastic pollution in the COVID-19 scenario. Mar. Pollut. Bull. *159*, 111517.

143. Fadare, O.O., and Okoffo, E.D. (2020). Covid-19 face masks: a potential source of microplastic fibers in the environment. Sci. Total Environ. *737*, 140279.

144. Lv, D., Zhu, M., Jiang, Z., Jiang, S., Zhang, Q., Xiong, R., and Huang, C. (2018). Green electrospun nanofibers and their application in air filtration. Macromol. Mater. Eng. *303*, 1800336.